A thermogravimetric study of the reactions of molybdenum disilicide with anhydrous hydrogen fluoride and fluorine

J.S. Gama [a,*], J.B. Wagener [a], P.L. Crouse [b]

[a] Applied Chemistry Department, The South African Nuclear Energy Corporation Ltd. (Necsa), P.O. Box 582, Pretoria 0001, South Africa [b] Department of Chemical Engineering, University of Pretoria, Pretoria 0002, South Africa

*Corresponding author. Tel.: +27 12 305 6135; fax: +27 12 305 3197. E-mail address: jabulani.gama@necsa.co.za (J.S. Gama).

ABSTRACT

The results of a thermogravimetric study into the dry fluorination of molybdenum disilicide, $MoSi_2$, using hydrogen fluoride and dilute fluorine gas as fluorinating agents are reported. The reaction between molybdenum disilicide and fluorine follows the thermodynamically preferred route, *viz*. the formation of the volatile molybdenum hexafluoride along with gaseous silicon tetrafluoride, with the reaction starting just below 200 °C. The reaction with hydrogen fluoride yields solid molybdenum metal and gaseous silicon tetrafluoride, similarly thermodynamically predicted, above 250 °C. No reaction is observed at low temperatures where solid molybdenum trifluoride is expected to form. The results of a kinetic analysis of the data for the reaction with hydrogen fluoride are reported. In the range 250–450 °C the kinetics are chemical reaction controlled. Above this, up to 700 °C, the rate is controlled by diffusion through the stagnant gas films surrounding the solid particles. Evidence for a third, un-quantified, high-temperature mechanism is given.

Keywords: Molybdenum disilicide Anhydrous hydrogen fluoride Thermogravimetric analysis Kinetics

1. Introduction

Four molybdenum fluorides are known to exist, *viz*. MoF_3, MoF_4, MoF_5 and MoF_6 [1–4], but only MoF_6 has commercial applications, primarily in the electronics industry [5]. Usually the volatile, hygroscopic molybdenum hexafluoride (MoF_6) is formed by reacting molybdenum metal with strong fluorinating agents, such as F_2, BrF_3, and SF_6 [6]. Exploding molybdenum metal into SF_6 gives a conversion of more than 70% to MoF_6, depending on the SF_6/Mo ratio, while non-volatile MoF_3 was reported to be present in minor quantities [1].

In most cases the lower molybdenum fluorides (MoF_3, MoF_4, and MoF_5) are formed through the reduction of high oxidation state metal fluorides [7].

However, it has been shown that the treatment of $MoSi_2$ with gaseous fluorine in the presence of tungsten (as an auxiliary substance) and sulphur (as a fuse) achieve complete conversion of $MoSi_2$ to MoF_6 and SiF_4 [8]. The objective of this work was to determine the enthalpy of formation of $MoSi_2$ at a specific temperature and pressure.

Molybdenum silicides ($MoSi_2$, Mo_3Si, and Mo_5Si_3) are known forhightemperatureapplications,becauseofphysicalproperties such as high melting points, super high oxidation resistance, formation of a thin protective surface silica layer (SiO2), and a high creep resistance [9–12]. Very little is known of the fluorination of molybdenum silicides using anhydrous hydrogen fluoride (AHF) or fluorine.

Thus, in this article we present results on the fluorine chemistry of molybdenum disilicide ($MoSi_2$) using thermogravimetry as tool, where $MoSi_2$ was treated with both fluorine and anhydrous hydrogen fluoride, without using any material as a fuse or as an auxiliary substance.

Equilibrium thermodynamic calculations predict that stoichiometric ratios of $MoSi_2$ and F_2 should produce $MoF_6(g)$ and $SiF_4(g)$ at all temperatures up to 1000 °C (Eq. (1)).

$$MoSi_2(s) + 7F_2(g) \rightarrow MoF_6(g) + 2SiF_4(g) \quad (1)$$

In the case of the reaction with HF, the equilibrium thermodynamic calculation with a stoichiometric ratio of 1:8 $MoSi_2$/HF predicts the formation of molybdenum metal, silicon tetrafluoride and hydrogen gas (Eq. (2)). While with excess HF (1:11 $MoSi_2$/HF), the equilibrium of thermodynamic calculation (Fig. 1) predicts the same products as above 80 °C, but below 80 °C MoF_3 should form as shown in Eq. (3).

$$MoSi_2 + 8HF(g) \rightarrow Mo + 2SiF_4(g) + 4H_2(g) \quad (2)$$

$$MoSi_2 + 11HF(g) \rightarrow MoF_3(s) + 2SiF_4(g) + 5.5H_2(g) \quad (3)$$

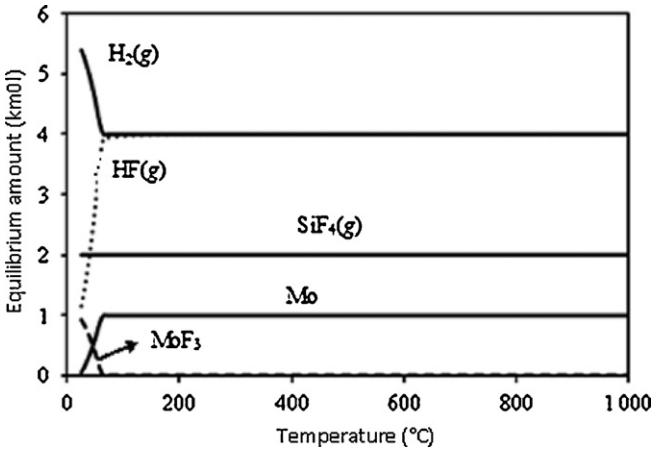

Fig. 1. Equilibrium composition for the reaction between $MoSi_2$ and HF (1:11 mol/mol).

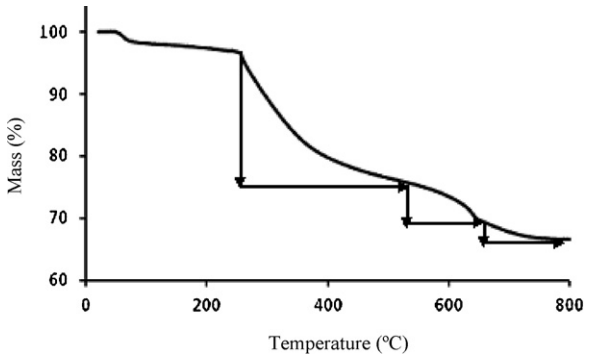

Fig. 3. Dynamic thermogravimetric curve of the reaction between $MoSi_2$ and 10% HF in nitrogen.

2. Results and discussion

The dynamic thermogravimetric fluorination of $MoSi_2$ with F_2 indicates that fluorine completely converts $MoSi_2$ into the volatile fluorides MoF_6 and SiF_4 (Fig. 2). Once the ignition temperature of about 180 °C has been achieved, the reaction proceeds easily to yield the volatile products and is complete at 330 °C. This result corresponds well with the thermodynamic prediction (Eq. (1)).

The dynamic thermogravimetric reaction between $MoSi_2$ and 10% AHF in nitrogen started with a small mass loss of about 2% (Fig. 3). This is possibly due to the removal of the silicon oxide layer (SiO_2), which forms when $MoSi_2$ is exposed to the atmosphere. After what appears to be an induction phase, full ignition is achieved at about 250 °C. The thermogravimetric curve suggests three distinct regimes, roughly in the ranges 250–550 °C, 550–650 °C, and 650–800 °C.

These three regimes resulted in a mass loss of about 31%, with a total mass loss of about 33%, as compared to the calculated 37.1% of a full conversion to Mo metal (Eq. (2)). Analysis of the final product by X-ray diffraction (XRD) showed molybdenum metal as the major phase. X-ray fluorescence (XRF) also showed trace amounts of silicon.

When the HF reactions were conducted isothermally (Fig. 4) in the temperature range of 200–700 °C, the theoretical mass loss of 37.1% was also not obtained. In this case only two regimes were observed. The mass loss increased as the temperature was increased, with the reactions at 600 °C and 700 °C having the highest mass loss of 32.7%. Molybdenum metal was the major phase by XRD analyses only at 700 °C. In the temperature range of 200–600 °C, $MoSi_2$ was the major phase, indicating incomplete fluorination of $MoSi_2$.

Scanning electron microscope (SEM) images of the product at different temperatures are given in Fig. 5. At 200 °C and 300 °C no major morphological changes are evident, which can be ascribed to the incomplete fluorination of $MoSi_2$. At 700 °C, where molybdenum metal was the major phase there are clear changes and particle shrinkage observed (Fig. 5).

To understand the mechanism of the regimes observed in Figs. 3 and 4, kinetic parameters were extracted. A number of kinetic models are possible for fluid–solid reactions, in this case the following assumptions were made: the particles are spherical and the reaction occurs first at the outer surface of the $MoSi_2$ particles, with the zone of the reaction moving toward the center, leaving behind completely converted material and unert solid. Therefore, at anytime there is an unreacted core of material which shrinks in size during the reaction. Thus for this work the three models of the shrinking core (SCM) were considered (Table 1). The three models with their fractional residue, α, as a function of time, are listed in Table 1. The full derivation of these models can be found in, *e.g.* Levenspiel [13]. Note that α is the fractional residue, not the extent of reaction. In all cases, ρ_B, is the molar density of the solid reactant, R is the initial particle size (assuming full sphericity), and C_g is the reactant gas concentration. In addition, k'' is the chemical reaction rate constant, k_g is the mass transport coefficient through the

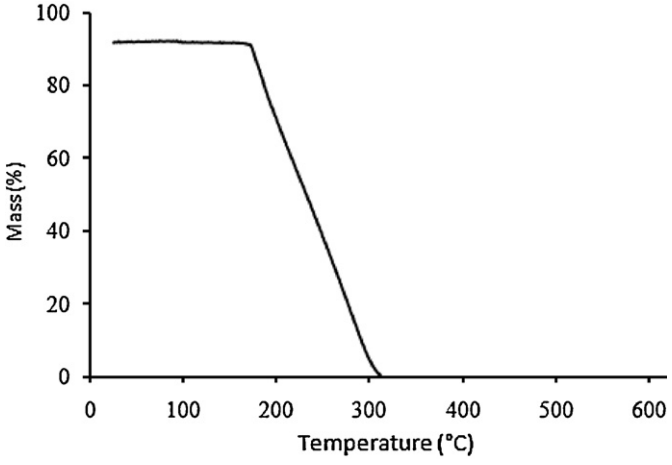

Fig. 2. Dynamic thermogravimetric curve of the reaction between $MoSi_2$ and 10% F_2 in nitrogen.

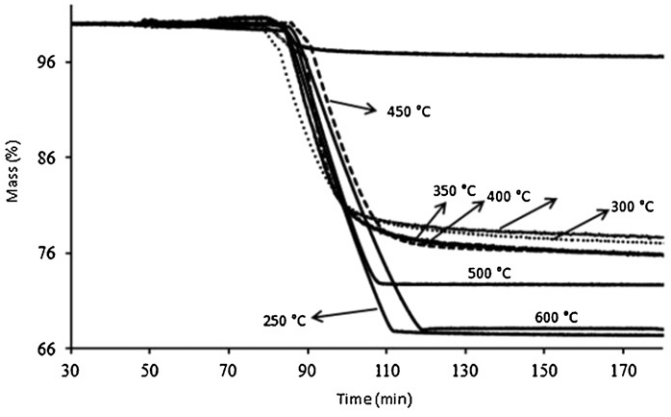

Fig. 4. Isothermal thermogravimetric curves of the reaction between $MoSi_2$ and 10% HF in nitrogen.

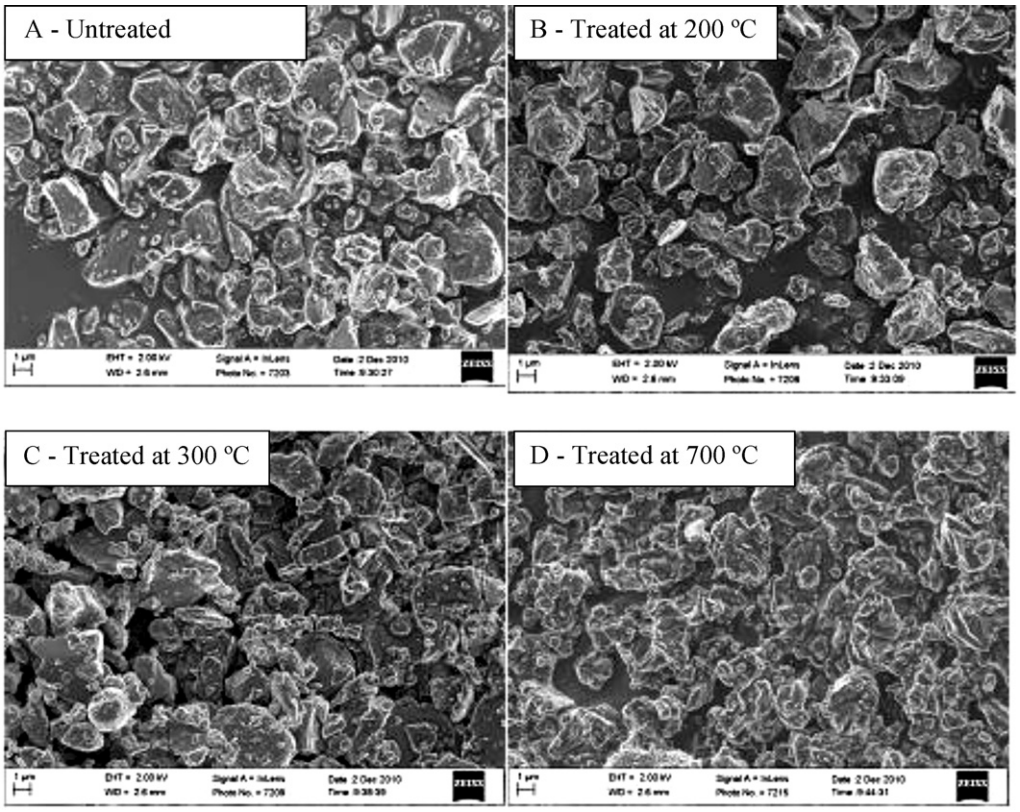

Fig. 5. SEM micrographs of $MoSi_2$, untreated and after reaction with HF at different temperatures.

stagnant gas film, and D_e is the effective diffusion constant through the product layer. The symbol b is the stoichiometric coefficient for the general gas–solid reaction:

$$A(g) + bB(s) \rightarrow \text{Products} \quad (4)$$

For model fitting purposes, the fractional residue, α, was referenced to the amount of silicon present. That is, m_0, the initial sample mass was taken as the mass of silicon present in the silicide, m_f was taken as the final mass of silicon present after the reaction. The time-dependent mass was taken as the sample mass minus the mass of metal (Mo) present. The span of α is thus 1 to 0 in each case, and since the LHS of the model equation tend to zero at $t = \tau$, the linear data plots were done for a zero y-intercept in each case.

$$\alpha = \frac{m_0}{m_f} \quad (5)$$

None of the models tested gave a good fit at 200 °C with R^2 values of 0.9161, 0.9141 and 0.8526, suggesting that the reaction only fully develops somewhat above 200 °C. Between 250 °C and 450 °C a better fit was obtained for chemical reaction control, while in the high-temperature region a better fit was obtained for gas-film diffusion control (Table 2).

Overall, the ash-layer control model fitted poorly in all cases. In the temperature range investigated, only two overlapping mechanisms could be identified, which corresponds to the first two regimes in Fig. 3. Between 250 °C and 450 °C, it appears that the chemical reaction itself controls the process, while between 450 °C and 700 °C, diffusion through the stagnant gas film surrounding the particles seems to be rate controlling. The third regime observed in the dynamic TG run for the reaction of HF with $MoSi_2$ (Fig. 3), evidently takes place at a temperature above this and could not be identified from the isothermal results. The Arrhenius parameters (activation energies and pre-exponential factors) are given in Table 3.

Table 1
Gas–solid reaction models evaluated.

Model	$f(\alpha)$	τ
Chemical reaction control	$1-\alpha^{1/3}=\frac{t}{\tau}$	$\tau=\frac{\rho_B R}{bk''C_g}$
Control by diffusion through stagnant gas film	$1-\alpha=\frac{t}{\tau}$	$\tau=\frac{\rho_B R}{3bk_gC_g}$
Control by diffusion through product layer	$1-3\alpha^{2/3}+2\alpha=\frac{t}{\tau}$	$\tau=\frac{\rho_B R^2}{6bD_eC_g}$

Table 2
R-Square values for better fit.

Model	R^2	
	250–450 °C	500–700 °C
Chemical reaction control	0.999	0.689
Diffusion through product layer	0.680	
Diffusion through stagnant gas film	0.654	0.911

Table 3
Arrhenius parameters.

Model	E_a (kJ/mol)	Pre-exponential factor ($m\,s^{-1}$ or $m^2\,s^{-1}$)
Chemical reaction control	29.54	0.032
Diffusion through stagnant gas film	12.56	0.329

3. Conclusions

$MoSi_2$ can be fully converted to MoF_6 and SiF_4 by reacting with dilute elemental fluorine. The reaction with gaseous HF only fully develops above 250 °C, and yields pure molybdenum metal along with SiF_4 at high temperatures (700 °C). Three kinetic regimes were detected in the dynamic thermogravimetric reaction with HF in three different temperature ranges (250–450 °C, 500–700 °C and above 700 °C). Arrhenius parameters for the first two of these regimes could be extracted from the isothermal thermogravimetric results.

4. Experimental

4.1. Materials

The molybdenum disilicide was purchased from Sigma–Aldrich. The dilute anhydrous hydrogen fluoride and fluorine gas (10% HF or F_2 diluted in N_2) were obtained from Pelchem (Pty) Ltd. All reagents had a purity of >99%.

4.2. Experimental procedure

An adapted thermogravimetric analyzer (TGA) was used for conducting the experiments. The instrument was modified to handle the corrosive gases HF and fluorine. Details are given in Gama et al. [14]. A starting mass of 40–60 mg $MoSi_2$ was used for each set of experiments. The $MoSi_2$ was stored in a glove box under nitrogen and treated with special consideration to minimize the oxygen present, even though $MoSi_2$ is known as reasonably oxidation resistant. Two thermogravimetric methods were used, *viz.* non-isothermal (dynamic) and isothermal. For isothermal experiments the sample was first heated to the predetermined temperature and then maintained at this constant temperature to equilibrate before introducing the reactive gas. For non-isothermal experiments the reactive gas was introduced at the beginning of each reaction and a heating rate of 10 °C/min was used. Isothermal experiments were only carried out with HF(g), since the fluorine reaction was considered to be of less interest.

The isothermal reactions were done at temperatures ranging between 200 °C and 700 °C. The samples were placed and heated in a small TG pan (inside diameter of 5.6 mm and a height of 1.6 mm) to the desired temperature using a rate of 10 °C/min. The diameter of the furnace tube was 10 mm. The thermocouple was inserted through the inlet of the reactive gas below the sample, and positioned just underneath the TG pan to accurately measure the temperature. The reactive gases were introduced at a flow rate of 60 mL/min.

The products obtained from these reactions were analyzed using Bruker A-D8 Advanced XRD for phase identification, ZEISS Gemini Ultra Plus Field Emission Gun (FEG) SEM for image analysis and EDX and Panalytical Axios XRF spectrometer for elemental analysis.

Acknowledgements

The South African Nuclear Energy Corporation (Necsa) in whose laboratories the work was done, the Graduate-in-Training (GIT) program at Necsa, and the financial support of the South African National Research Foundation (NRF) are gratefully acknowledged by the authors. Mr. B.M. Vilakazi of Necsa is acknowledged for his assistance in obtaining the thermogravimetric data.

References

[1] R.L. Johnson, B. Siegel, Journal of Inorganic and Nuclear Chemistry 31 (1968) 663–955.
[2] D.E. LaValle, R.M. Steele, M.K. Wilkinson, H.L. Yaker Jr., Journal of the American Chemical Society 82 (1960) 2433–2434.
[3] F.A. Cotton, G. Wilkinson, Advanced Inorganic Chemistry, 4th edition, John Wiley and Sons, New York, 1962.
[4] M.L. Larson, F.W. Moore, D.A. Edwards, Inorganic Synthesis 12 (1970) 165–178.
[5] K. Bjorklund, Microfabrication of Tungsten, Molybdenum ans Tungsten Carbide Rods by Laser-assisted CVD, ACTA Universitatis upsaliensis, Uppsala, Sweden, 2001 http://uu.diva-portal.org/smash/record.jsf?pid=diva2:161180.
[6] O. Glemser, Journal of Fluorine Chemistry 33 (1986) 45–69.
[7] R.B. Heslop, P.L. Robinson, Inorganic Chemistry, Elsevier, Amsterdam, 1967.
[8] P.A.G. O'Hare, Journal of Chemical Thermodynamics 25 (1993) 1333–1343.
[9] Z. Yao, J.J. Stiglich, T.S. Sudarshan, Journal of Materials Engineering and Performance 8 (1999) 291–304.
[10] N.N. Greenwood, A. Earnshaw, Chemistry of the Elements, Elsevier, Oxford, 1984 .
[11] K. Natesan, S.C. Deevi, Intermetallics 8 (1999) 1147–1158.
[12] V.A. Maksimov, Inorganic Materials (Neorganicheskie Materialy) 5 (1996) 965–966.
[13] O. Levenspiel, Chemical Reaction Engineering, John Wiley, New York, 1996.
[14] J.S. Gama, J.B. Wagener, P.L. Crouse, Journal of Fluorine Chemistry 139 (2012) 12–15.